Biomedicine & Pharmacotherapy 143 (2021) 112217

Contents lists available at ScienceDirect

Biomedicine & Pharmacotherapy

journal homepage: www.elsevier.com/locate/biopha

Urinary metabolomics of HCV patients with severe liver fibrosis before and during the sustained virologic response achieved by direct acting antiviral treatment

Elisa Biliotti [a,1], Ottavia Giampaoli [b,c,1], Fabio Sciubba [b,c], Federico Marini [b,c], Alberta Tomassini [b,c], Donatella Palazzo [a], Giorgio Capuani [b,c], Rozenn Esvan [a], Martina Spaziante [a], Gloria Taliani [a], Alfredo Miccheli [c,d,*]

[a] Department of Translational and Precision Medicine, Sapienza University of Rome, Rome, Italy
[b] Department of Chemistry, Sapienza University of Rome, Rome, Italy
[c] NMR-based Metabolomics Laboratory (NMLab), Sapienza University of Rome, Rome, Italy
[d] Department of Environmental Biology, Sapienza University of Rome, Rome, Italy

ARTICLE INFO

Keywords:
NMR-based metabolomics
hepatitis C virus (HCV)
direct-acting antivirals (DAAs)
Oxidative stress
amino acid metabolism

ABSTRACT

Hepatitis C virus (HCV) infection induces a long-term inflammatory response and oxidative-stress in the liver microenvironment, leading to hepatic fibrosis and metabolic alterations. Direct-acting-antiviral-agents (DAAs) induce HCV-clearance, even though liver damage is only partially restored. In this context, understanding the impact of viral-eradication on liver metabolic activities could allow optimizing the metabolic care of the patient. The present prospective longitudinal study aims at characterizing the urinary metabolic profile of HCV-induced severe liver fibrosis and the metabolic changes induced by DAAs and HCV-clearance by nuclear magnetic resonance-based metabolomics. The urinary metabolic profile of 23 HCV males with severe liver fibrosis and 20 age-matched healthy-controls was analyzed by NMR-based-metabolomics before starting DAAs, at the end-of-therapy, after one and three months of follow-up. The urinary metabolic profile of patients with severe liver fibrosis was associated to pseudouridine, hypoxanthine, methylguanidine and dimethylamine, highlighting a profile related to oxidative damage, and to tyrosine and glutamine, related to a decreased breakdown of aromatic aminoacids and ammonia detoxification, respectively.

1-methylnicotinamide, a catabolic intermediate of nicotinamide-adenine-dinucleotide, was significantly increased in HCV-patients and restored after HCV-clearance, probably due to the reduced hepatic inflammation. 3-hydroxy-3-methylbutyrate, an intermediate of leucine-catabolism which was permanently restored after HCV-clearance, suggested an improvement of skeletal muscle protein synthesis. Finally, 3-hydroxyisobutyrate and 2,3-dihydroxy-2-methylbutyrate, intermediates of valine-catabolism, glycine and choline increased temporarily during therapy, resulting as potential biomarkers of DAAs systemic effects.

1. Introduction

Chronic hepatitis C (CHC) represents a public health problem, affecting more than 71 million of individuals worldwide with an estimated global prevalence of 1% [1]. Hepatitis C virus (HCV) infection causes liver inflammation and progressive liver fibrosis, leading to cirrhosis and its complications, such as portal hypertension, liver decompensation and hepatocellular carcinoma (HCC). Consequently, CHC is a leading cause of liver-related morbidity and mortality, accounting for nearly 500.000 related deaths per year [2]. In addition, CHC is a systemic infection that can lead to extrahepatic manifestations, including cryoglobulinaemia, kidney disease, non-Hodgkin lymphoma, cardiovascular disease, insulin-resistance and diabetes [3].

For many years, the treatment for CHC involved the use of interferon, whose antiviral action consisted in a progressive immune-mediated elimination of infected hepatocytes [4]. Recently, direct-acting

* Correspondence to: Department of Environmental Biology, Sapienza University of Rome, Piazzale Aldo Moro, 5, 00185 Rome, Italy.
E-mail address: alfredo.miccheli@uniroma1.it (A. Miccheli).
[1] Contributed equally to this article.

https://doi.org/10.1016/j.biopha.2021.112217
Received 17 May 2021; Received in revised form 14 September 2021; Accepted 16 September 2021
Available online 21 September 2021

antiviral agents (DAAs), which inhibit critical steps in the HCV replication cycle, have revolutionized the treatment landscape with very high cure rates (over 95%), short treatment duration (8–24 weeks), excellent tolerability and low treatment failure [5,6]. It has been suggested that DAAs induce not only hepatocyte elimination, but also a progressive reduction of intracellular viral content down to its disappearance (cell cure), leading to a fast improvement of liver homeostasis [7].

Although patients with severe liver fibrosis, who achieve a sustained virologic response (SVR) by means of DAAs, experience a reduction of mortality and liver-related complications, the risk of HCC occurrence persists over time [8] and the reversibility of some liver-related and extrahepatic manifestations remains an unclarified issue. Therefore, understanding the impact of DAA treatment and HCV clearance on the metabolic liver activities may lead to the optimization of metabolic care of subjects with severe liver fibrosis during treatment and follow-up.

Liver is a major organ with several metabolic activities, including amino acid and glucose metabolism. Several conditions perturb regulation of liver metabolism. From this point of view, the blood or urine metabolic profiling should represent the final outcome of liver cellular regulation at many different levels, and, for this reason, the phenotypic response to a disease or its treatment [9].

Metabolomics provides a snapshot of a full set of metabolites (called metabolome) detected in biofluids, as urine or plasma, at a given time, allowing a systemic overview of the organism physiology both in health and disease. Nuclear Magnetic Resonance (NMR) is one of the main analytical platforms used in metabolomics: it is a specific, reproducible and non-invasive technique. It allows the identification and quantification of the more abundant compounds in a biological fluid without time-consuming sample preparation and fractionation. NMR-based metabolomics has been widely used in liver disease studies and urinary NMR-based metabolomics has been applied as a tool to investigate different hepatic diseases [9–15]. The application of metabolomics for studying patients with HCV infection could be decisive in understanding pathological processes.

This study represents the first investigation that monitors the metabolic changes occurring in HCV patients with severe liver fibrosis before and at the end of DAA therapy and during three months of follow-up by urinary ^{1}H NMR-based metabolomics. The aim of this work is to define the characteristic metabolic profile of HCV-induced severe liver fibrosis, to evaluate the metabolic changes due to DAA therapy and the metabolic effects of HCV clearance.

2. Materials and methods

2.1. Patients' characteristics, enrollment and antiviral regimens

All consecutive patients who received DAA treatment for HCV infection at the Liver Diseases Unit, Policlinico Umberto I in Rome, from January to December 2015 were evaluated for participating in the study. Inclusion criteria were: 1) age $\geq$ 18 years 2) diagnosis of severe liver fibrosis or cirrhosis. Exclusion criteria were: 1) female gender 2) evidence of autoimmune hepatitis or alcoholic liver disease 3) malignancies, 4) coinfection with HBV or HIV, 5) Child-Pugh classes B and C cirrhosis 6) HCV genotype other than 1 7) diabetes 8) estimated glomerular filtration rate (e-GFR) $\leq$ 60 mL/min/1.73 m^2.

The patient enrollment flow chart is reported in Fig. 1. One hundred and thirty consecutive HCV patients were evaluated for participating in the study. One hundred and seven patients were excluded because 50 were women and 57 had one or more exclusion criteria (HIV coinfection, diabetes, e-GFR $\leq$ 60 mL/min/1.73 m^2, HCV genotype other than 1, Child-Pugh B or C cirrhosis). Finally, 23 male patients with severe liver fibrosis were enrolled in the study.

Age, gender, body mass index (BMI), arterial pressure, severity of liver fibrosis, complete blood count, liver function tests, Homeostasis Model Assessment Insulin Resistance (HOMA-IR) and e-GFR were assessed in all patients at baseline (BT0), end of treatment (EOT) and three months after EOT (FU3). In addition, a hepato-splenic ultrasound and a transient elastography (*Fibroscan*) were performed before the enrollment in the study and six months after the end of the therapy (FU-6).

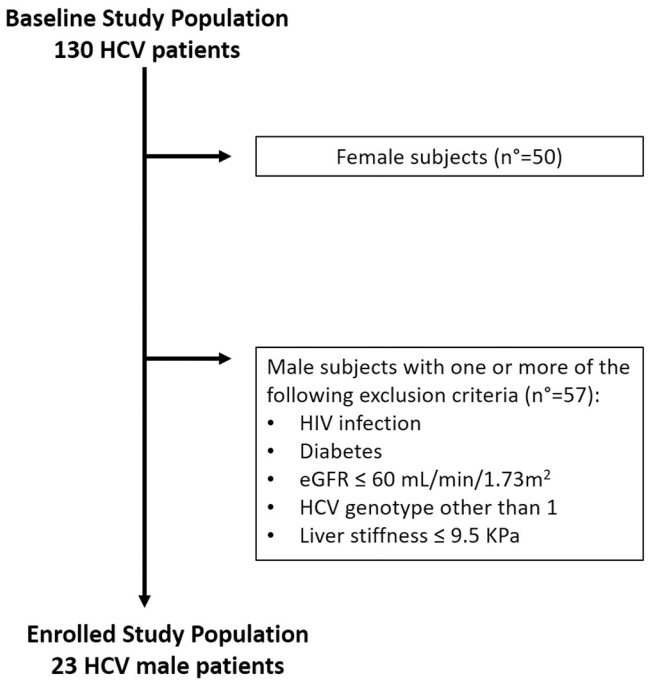

Fig. 1. Flow-chart of the enrollment of HCV patients.

The presence of advanced fibrosis and cirrhosis was defined as a liver stiffness value higher than 9.5 KPa and 12.5 KPa, respectively [16]. E-GFR was evaluated using Chronic Kidney Disease Epidemiology Collaboration Formula (CKD-EPI-2009 formula).

Treatment regimens were chosen according to the Italian guidelines and to the availability of different regimens over time. Treatments included: 1) sofosbuvir and ledipasvir with or without ribavirin 2) paritaprevir/ritonavir, ombitasvir and dasabuvir with or without ribavirin 3) sofosbuvir and simeprevir with or without ribavirin. The treatment duration varied from 12 to 24 weeks according to the infecting genotype and ribavirin use. Dose adjustments, treatment interruption and adherence were recorded. SVR was defined as serum HCV-RNA undetectability 12 weeks after EOT.

2.2. ^{1}H NMR spectroscopy

The urinary metabolic profiles of 23 enrolled HCV patients were evaluated at BT0, EOT, after one month from EOT (FU1) and after three months from EOT (FU3). At each time point, the urinary metabolic profile of HCV patients was compared to that of 20 age-matched male healthy controls (CTRL).

2.2.1. Sample preparation

The first urines in the morning were collected from fasting subjects. Urine samples were centrifuged at 11,000×*g* for 15 min at 4 °C. One hundred microliters of a 3-trimethylsilyl-propionic-2,2,3,3-d4 acid (TSP) in cold phosphate-buffered saline–D_2O solution (2 mmol l^{-1} final concentration) were added, as internal standard, to 1000 µl of centrifuged urine. The pH of urine was measured and adjusted at pH 7 by adding NaOH or HCl. Finally, 600 µl of each sample were transferred to NMR tubes.

2.2.2. NMR acquisition and processing

^{1}H NMR spectra were acquired at 298 K using a Bruker AVANCE III 400 spectrometer (Bruker BioSpin GmbH, Karlsruhe, Germany) equipped with a magnet operating at 9.4 Tesla, corresponding to a frequency of 400.13 MHz for ^{1}H. All the acquisition and processing parameters are reported elsewhere [17].

Signal assignments were achieved by standard two-dimensional (2D) ^{1}H–^{1}H Correlation Spectroscopy, Total Correlation Spectroscopy, ^{1}H–^{13}C Heteronuclear Single Quantum Correlation and Heteronuclear Multiple Bond Correlation on selected samples and confirmed by data base and literature comparison [2,3]. One-dimensional NMR spectra were processed by using the ACD Lab ^{1}D NMR Manager ver. 12.0 software (Advanced Chemistry Development, Inc., Toronto, ON, Canada), whereas ^{2}D NMR spectra were processed by using Bruker Top Spin ver. 3.1 (Bruker BioSpin GmbH). The NMR spectra were manually phased, baseline corrected and referenced to the chemical shift of the TSP methyl resonance at δ 0.00. The quantification of metabolites was made by comparing the specific signal integrals to the TSP integral. Metabolite levels were expressed as μmol mmol^{-1} creatinine, using the creatinine methylene group signal at 4.05 p.p.m. as a reference.

The study protocol conformed to the ethical guidelines of the 1975 Declaration of Helsinki and it was approved by the Institutional Review Board. All patients provided their written informed consent to participate in the study.

2.3. Statistical analysis

Multivariate and univariate analyses were applied in order to evaluate the metabolomic differences between HCV patients and healthy controls and the effects of the antiviral treatment.

Principal Component Analysis (PCA) was used for exploratory analysis to evidence possible clusters and outliers and was performed by using Unscrambler 10.5 software (CAMO, Oslo, Norway). The data were autoscaled before further data processing.

For the classification stage, different models were built using the Partial Least Square-Discriminant Analysis (PLS-DA) algorithm, and validated according to the strategy proposed by Szymańska et al. [18]. This approach, based on repeated double cross-validation (rDCV) coupled to permutation tests, allows estimating confidence intervals for the model predictions and assessing the stability/consistence of candidate biomarkers.

Each permutation test was performed based on 1000 randomizations. The area under the receiver operating characteristic (AUROC) curve was used to evaluate the quality and the predictive ability of the classification models. AUROC is a figure of merit borrowed from signal processing and is particularly useful to characterize binary classifiers. Its values range between 1 (perfect classification) and 0 (no discrimination). The accuracy, specificity and sensitivity of the models were also calculated, as additional figures of merit. Identification of the most relevant metabolites for the discrimination among the investigated classes was carried out by inspecting the values of their associated Variable Importance in Projection (VIP) indexes (VIP>1). Additionally, exploiting the advantage of having paired measurements on the same patients at BT0 and EOT stages, a multilevel PLS-DA approach was also adopted to evaluate the metabolic differences between the two conditions, after filtering out the inter-individual variability (by centering the metabolite levels measured at BT0 and EOT for any individual patient around their respective averages). PLS-DA models were calculated and validated by means of in-house written function running under MATLAB environment (R2015b; The MathWorks, Natick, MA) or by software.

Univariate evaluation of the variables identified as significant based on PLS-DA analysis was conducted performing Kruskal-Wallis test followed by Pairwise Multiple Comparison with Dunn's proposed Bonferroni correction. The metabolite levels measured on HCV patients at BT0, EOT, FU1, FU3 were compared to those of the corresponding metabolites in the urine of Ctrl. Univariate analysis was carried out by Sigma plot 14 (Systat Software, Palo Alto, CA).

3. Results

Twenty-three consecutive HCV male patients were enrolled in the study, 78.3% (18/23) of them had a compensated cirrhosis (Child-Pugh A5 or 6), while 21.7% (5/23) had advanced liver fibrosis. The baseline characteristics of the study population are shown in Supplementary Table 1. Mean age was 57.6 ± 9.0 years, mean BMI was 24.9 ± 3.3 kg/m^2 and the prevalence of arterial hypertension was 30.4% (7/23). Mean e-GFR was 96.9 ± 8.8 mL/min/1.73 m^2. All patients were HCV genotype 1 infected patients (69.6% genotype 1a, 30.4% genotype 1b).

Patients were treated with different interferon free regimens, 73.8% (17/23) of which including ribavirin (Supplementary Table 2). SVR was achieved in all patients.

Overall, a significant improvement of liver function tests occurred during DAA treatment, with a significant decrease of aspartate aminotransferase (AST), alanine aminotransferase (ALT) and gamma glutamyl transferase (γGT) values. Albumin values remained stable from baseline to EOT. A significant decrease of HOMA-IR was observed during therapy (4.6 vs. 3.3, $p = 0.004$), and remained stable during follow-up (Supplementary Table 3). The HOMA-IR values were positively correlated (Spearman correlation analysis) with the liver stiffness ($r = 0.63$, $p = 0.003$) measured on BT0 patients by Fibroscan. Fibroscan measurements were only performed at BT0 and FU-6, follow-up time which was not considered in this study because of the lack of the corresponding urinary metabolomic analysis. Therefore, it was not possible to assert whether this correlation was also maintained at EOT or not. Nevertheless, an associated trend of HOMA-IR and fibrosis improvement could still be inferred comparing Fibroscan data at BT0 and FU-6 (17.5 vs. 9.7, $p < 0.001$), indicating a percent decrease of 40% due to DAA treatment and SVR.

A representative urinary ^{1}H NMR spectrum of a patient is shown in Supplementary Fig. 1. Forty-four urinary metabolites were quantified from ^{1}H NMR spectra of 20 healthy controls (mean age 56.45±8.11 years) and 23 HCV patients at BT0, EOT, FU1 and FU3. The list of the identified and unassigned metabolites with the relative chemical shifts of the resonances is reported in Supplementary Table 4.

The data matrix included, as variables (columns), 44 urinary metabolites and, in the case of PLS-DA, three additional blood variables, namely AST, ALT and γGT. The resonances assigned to the compounds and metabolites of antiviral drugs were not included in the analysis. Firstly, we performed an explorative time trajectory PCA for patients at BT0, EOT, FU1 and FU3. The first two components explain a relatively low percentage of the total variance (around 25%) and a large confounding variability did not allow to observe a different spatial distribution of samples according to time course (Supplementary Fig. 2).

Based on these results, we decided to separately analyze the data matrix by PLS-DA in order to identify the urinary metabolic profiles of HCV patients with severe liver fibrosis in comparison to Ctrl (BT0 vs Ctrl) and the variation of urinary metabolic profile influenced by DAA treatment on HCV patients (EOT vs. BT0; EOT vs Ctrl).

In addition, the provisional or persistent nature of the discriminating metabolites has been evaluated by univariate analysis of the changes comparing metabolite levels of Ctrl and patients at BT0, EOT, FU1 and FU3.

3.1. Baseline metabolic profile of HCV patients compared to controls

A first PLS-DA was performed on the data matrix comparing Ctrl and HCV patient at BT0. The metabolic profiles of Ctrl and patients were well separated by inspecting the PLS-DA scores plot (Fig. 2A). The PLS-DA model showed 1 significant Latent Variable (LV). The validation results through rDCV and permutation test indicated an overall accuracy of 85.0 ± 3.2% ($p < 0.001$), and sensitivity and specificity values for the BT0 patients as compared to Ctrl of 78.9 ± 5.4% ($p < 0.001$) and

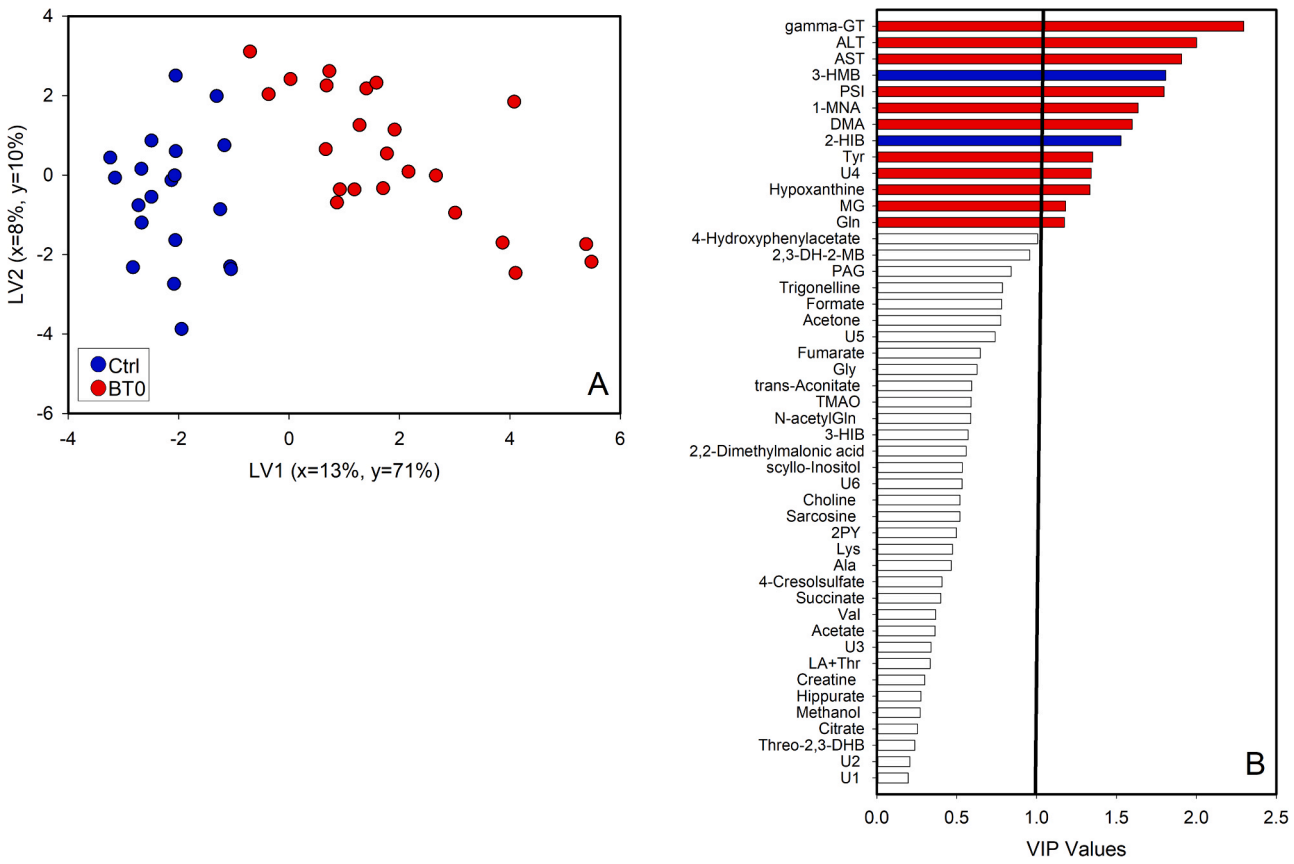

Fig. 2. PLS-DA analysis. A) Score plot for the paired metabolomics analysis of HCV patients at BT0 (red) and CTRL (blue); B) VIP values are reported in horizontal histograms and values of VIP upper to 1 are statistically significant. In red is indicated the metabolite that is higher in BT0, in blue the metabolite that is higher in Ctrl. Abbreviations: 1-MNA: 1-Methylnicotinamide; 2,3-DH-2-MB: 2,3-dihydroxy-2methylbutyrate; 2-HIB: 2-Hydroxyisobutyrate; 2PY: N-methyl-2-pyridone-5-carboxamide; 3-HIB: 3-hydroxyisobutyrate; 3-HMB: 3-Hydroxy-3-methylbutyrate; Ala: Alanine; ALT: Alanine aminotranferase; AST: Aspartate aminotranferase; DMA: Dimethylamine; Gln: Glutamine; Gly: Glycine; LA+Thr: Lactate+Threonine; Lys: Lysine; MG: Methylguanidine; N-acetylGln: N-acetylglutamine; PAG: Phenylacetylglycine; PSI: Pseudouridine; Threo-2,3-DHB: Threo-2,3-dihydroxybutyrate; TMAO: Trimethylamine-N-oxide; Tyr: Tyrosine; Val: Valine; γGT: Gamma glutamyl tranferase. For interpretation of the references to color in this figure legend, the reader is referred to the web version of this article.

91.4 ± 4.6% ($p = 0.003$), respectively. The AUROC value was 0.892 ± 0.029 (Supplementary Fig. 3A).

On the basis of the VIP values, nine metabolites were identified as significantly relevant for the discrimination. In particular, the levels of 3-hydroxy-3-methylbutyrate (3-HMB) were lower, while the levels of 2,3-dihydroxy-2-methylbutyrate (2,3-DH-2-MB), glutamine (Gln), dimethylamine (DMA), methylguanidine (MG), tyrosine (Tyr), pseudouridine (PSI), hypoxanthine, 1-methylnicotinamide (1-MNA) were higher in urine of HCV patients than in those of controls (Fig. 2B). These variations of urinary metabolites were associated with higher levels of AST, ALT and γGT.

The differences of 3-HMB, PSI, MG, 1-MNA and hypoxanthine levels observed between BT0 and Ctrl resulted to be also significant ($p < 0.05$) by Kruskal-Wallis analysis after Bonferroni correction (Dunn's method).

3.2. Metabolic profile of HCV patients at the end of DAA treatment compared to baseline

In order to evaluate the metabolic effect of DAA therapy, multi-level PLS-DA analysis was carried out comparing the metabolic profiles of HCV patients at EOT and BT0.

The multi-level PLS-DA model resulted in 1 significant Latent Variable (LV). The validation strategy conducted through rDCV and permutation test resulted in an overall accuracy of 99.3 ± 1.7% ($p < 0.001$), and in sensitivity and specificity values for EOT as compared to BT0 of, 99.8 ± 1.5% ($p < 0.001$) and 99.4 ± 1.6% ($p < 0.001$), respectively. The AUROC value was 0.999 ± 0.002 (Supplementary Fig. 3B).

VIP values showed fourteen significant variables characterizing the EOT metabolic profile of patients compared to BT0. Specifically, the levels of threo-2,3-dihydroxybutyrate (threo-2,3-DHB), 3-HMB, 3-HIB, 2,3-DH-2-MB, 2-HIBA, lactate+threonine (LA+Thr), glycine (Gly), 2,2-dimethylmalonic acid, choline and Tyr were higher in patients at EOT, while 1-MNA levels, serum AST, ALT and γGT were lower (Fig. 3A).

The differences of serum AST, ALT, γGT levels (Supplementary Table 3) and urinary 3-HMB, Tyr, 2,2-dimethylmalonic acid, and Gly levels observed between EOT and BT0 resulted to be also significant ($p < 0.05$) by Kruskal-Wallis analysis followed by Bonferroni correction (Dunn's method).

3.3. Metabolic profile of HCV patients at the end of DAA treatment compared to controls

In order to discriminate the metabolic effect of DAA therapy and HCV clearance, a further PLS-DA analysis was carried out comparing patients at EOT vs Ctrl.

The PLS-DA model showed 2 significant Latent Variable (LV). The validation strategy through rDCV and permutation test resulted in an overall accuracy of 87.7 ± 3.5% ($p < 0.001$), and sensitivity and specificity values for EOT as compared to Ctrl: of 82.6 ± 6.4% ($p < 0.001$) and 93.3 ± 3.3% ($p < 0.001$), respectively. The AUROC value was 0.928 ± 0.015 (Supplementary Fig. 3C).

In particular, HCV patients at EOT had significantly higher urinary levels of Tyr, U4, hypoxanthine, Gln, 2,3-DH-2-MB, PSI, choline, 3-HIB,

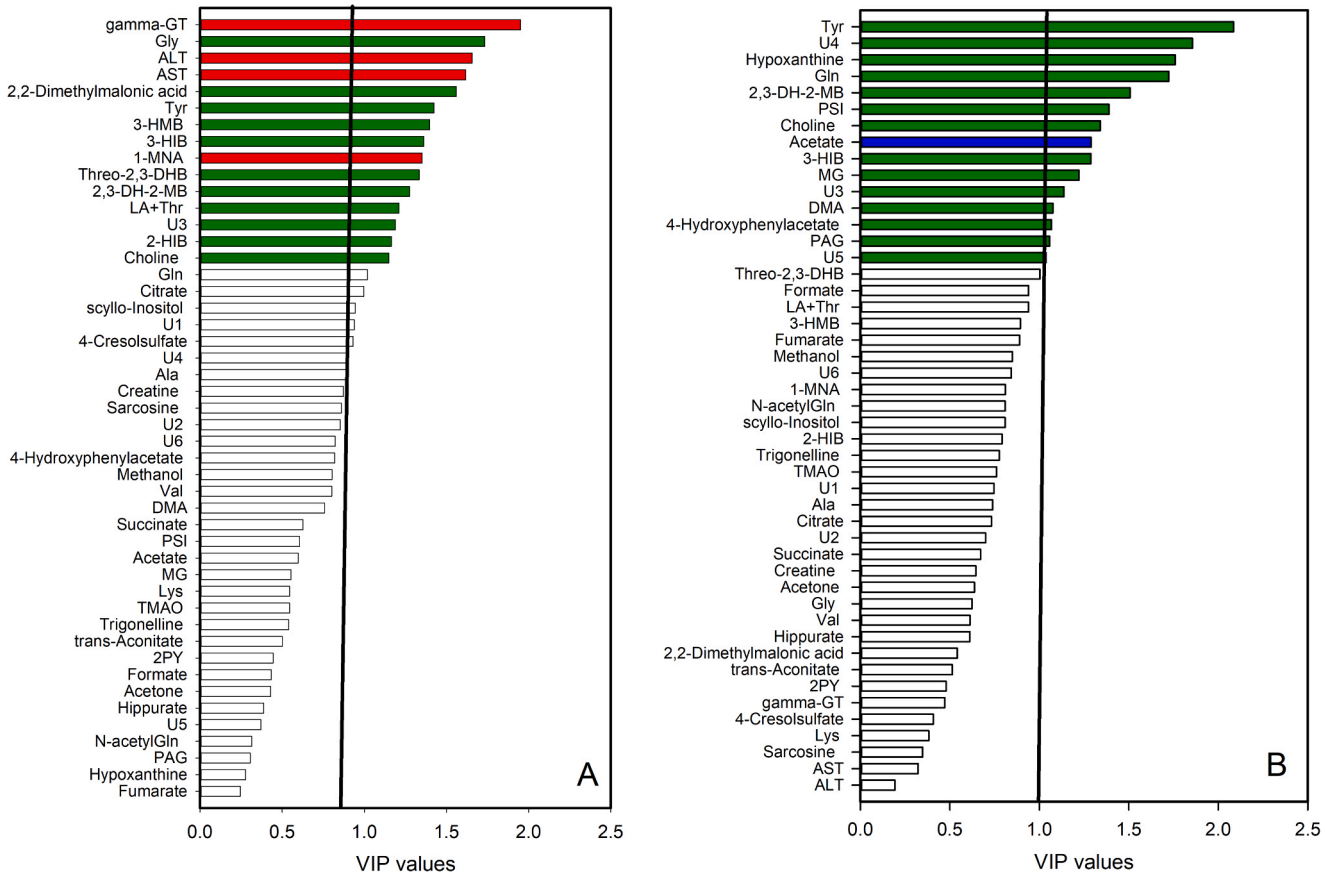

Fig. 3. VIP values reported in horizontal histograms from: A) Paired PLS-DA performed between patients at EOT and BT0. In green is indicated the metabolite that is higher in patients at EOT and in red the metabolite that is higher at BT0. B) PLS-DA performed between patients at EOT and Ctrl. In green is indicated the metabolite that is higher in patients at EOT and in blue the metabolite that is higher in Ctrl. Abbreviations: 1-MNA: 1-Methylnicotinamide; 2,3-DH-2-MB: 2,3-dihydroxy-2methylbutyrate; 2-HIB: 2-Hydroxyisobutyrate; 2PY: N-methyl-2-pyridone-5-carboxamide; 3-HIB: 3-hydroxyisobutyrate; 3-HMB: 3-Hydroxy-3-methylbutyrate; Ala: Alanine; ALT: Alanine aminotranferase; AST: Aspartate aminotranferase; DMA: Dimethylamine; Gln: Glutamine; Gly: Glycine; LA+Thr: Lactate+Threonine; Lys: Lysine; MG: Methylguanidine; N-acetylGln: N-acetylglutamine; PAG: Phenylacetylglycine; PSI: Pseudouridine; Threo-2,3-DHB: Threo-2,3-dihydroxybutyrate; TMAO: Trimethylamine-N-oxide; Tyr: Tyrosine; Val: Valine; γGT: Gamma glutamyl tranferase. For interpretation of the references to color in this figure legend, the reader is referred to the web version of this article.

MG, U3, DMA, 4-hydroxyphenylacetate, PAG, U5 as compared to CTRL (Fig. 3B), while acetate was lower in EOT patients. Furthermore, Tyr, hypoxanthine, Gln, 2,3-DH-2-MB, PSI, choline, 3-HIB, MG, DMA, 4-hydroxyphenylacetate, U3, U4 were significantly higher in EOT patients than in Ctrl, according to Kruskal-Wallis analysis with Bonferroni correction (Dunn's method).

3.4. Urinary biomarkers correlated to severe liver fibrosis, SVR and DAA administration

In order to highlight the drug metabolic effects, the evolution of the changes of the significant metabolic variables by PLS-DA were investigated at FU1 and FU3. Furthermore, these selected variables were compared to the levels observed in the Ctrl to evaluate a possible restoration to the normal range. Three groups of urinary metabolites were identified according to the results of univariate statistical analysis and of the similarity among their time evolution: i) urinary biomarkers related to severe liver fibrosis and not influenced by the DAA treatment or HCV clearance: PSI, hypoxanthine, MG, DMA, Tyr, Gln (Fig. 4). Tyr and Gln showed a peculiar behavior, since their levels were significantly higher in HCV patients at BT0 and EOT compared to Ctrl, increased significantly during the DAA treatment and remained stable during follow-up; ii) urinary biomarkers associated with HCV clearance and SVR which responded to DAA treatment and returned to Ctrl levels at EOT without further changes during follow-up: 1-MNA and 3-HMB (Fig. 5); iii) urinary biomarkers related to DAA treatment which varied during antiviral therapy and returned to BT0 levels at follow-up: 3-HIB, 2,3-DH-2-MB and Gly (Fig. 6). The changes of these metabolites were not influenced by the type of DAA regimen. Specifically, patients treated with an antiviral regimen including a protease inhibitor (PI) (simeprevir or paritaprevir/ritonavir) experienced similar changes of these metabolites compared to those treated with regimen not including PI (data not shown).

4. Discussion

Several metabolomic studies have been conducted in patients with HCV infection aimed at finding serum biomarkers of liver fibrosis progression and HCC development [14,15,19,20]. To the best of our knowledge, the present prospective longitudinal study is the first to comprehensively investigate, by NMR-based metabolomics, the urinary metabolic changes in HCV patients with advanced severe liver fibrosis during DAAs treatment and follow-up.

In this study, metabolic profiling allowed us to characterize the urinary metabotype of CHC patients and to monitor the changes during the course of the therapy, disentangling the metabolic effects due to severe liver fibrosis from those depending on viral clearance and on the systemic effects induced by DAA therapy.

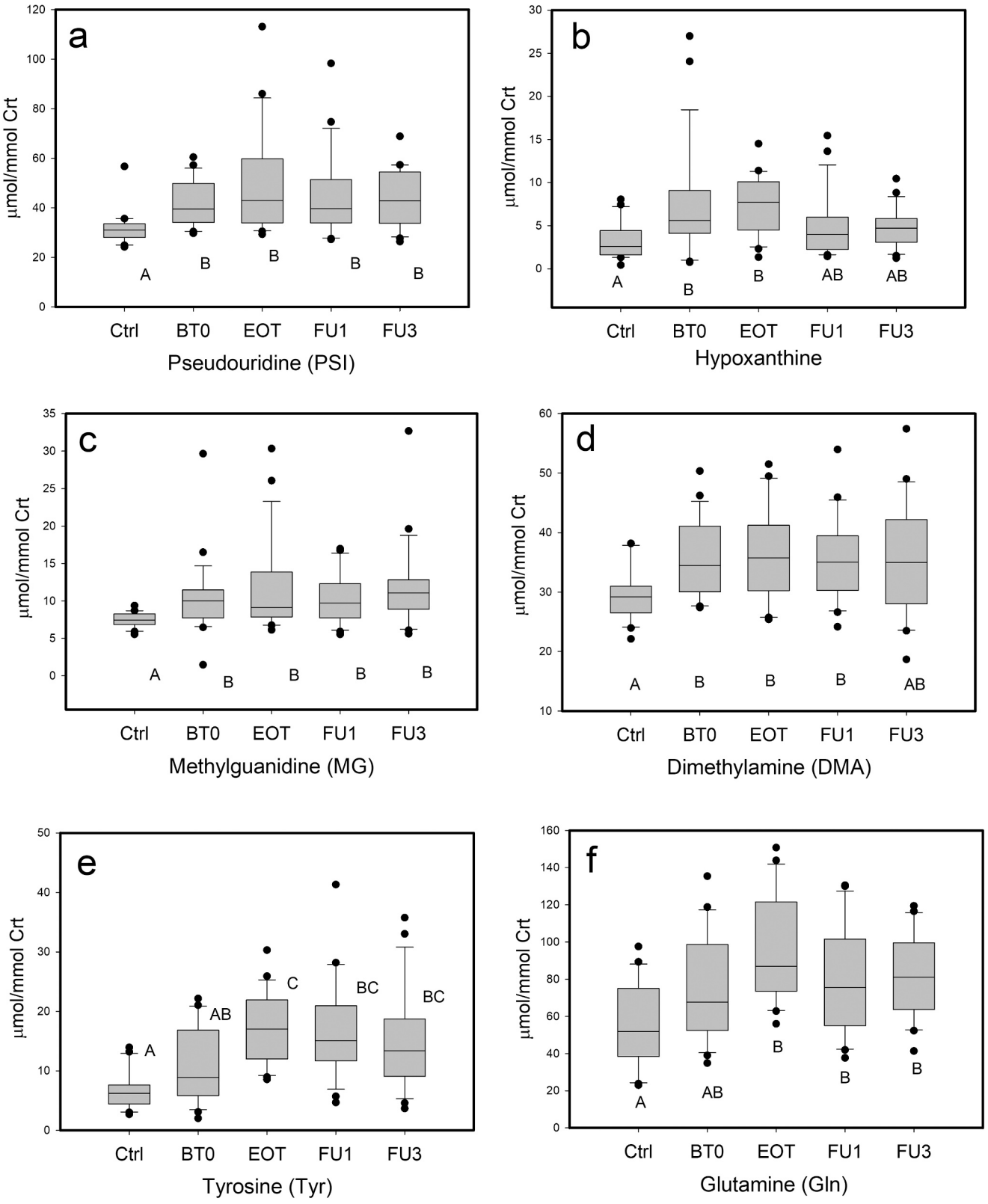

Fig. 4. Boxplot of urinary biomarkers related to severe liver fibrosis: a) PSI, b) Hypoxanthine, c) MG, d) DMA, e) Tyr, f) Gln. Statistical significance was assessed by Kruskal-Wallis ANOVA on ranks test, using Bonferroni correction for P values (Dunn's method). P-value of 0.05 was considered as threshold for statistical significance, which is reported as letters (A or B or C) on the boxplots. Same letters indicate that there is no statistically significant difference, different letters indicate that there is a statistically significant difference among groups.

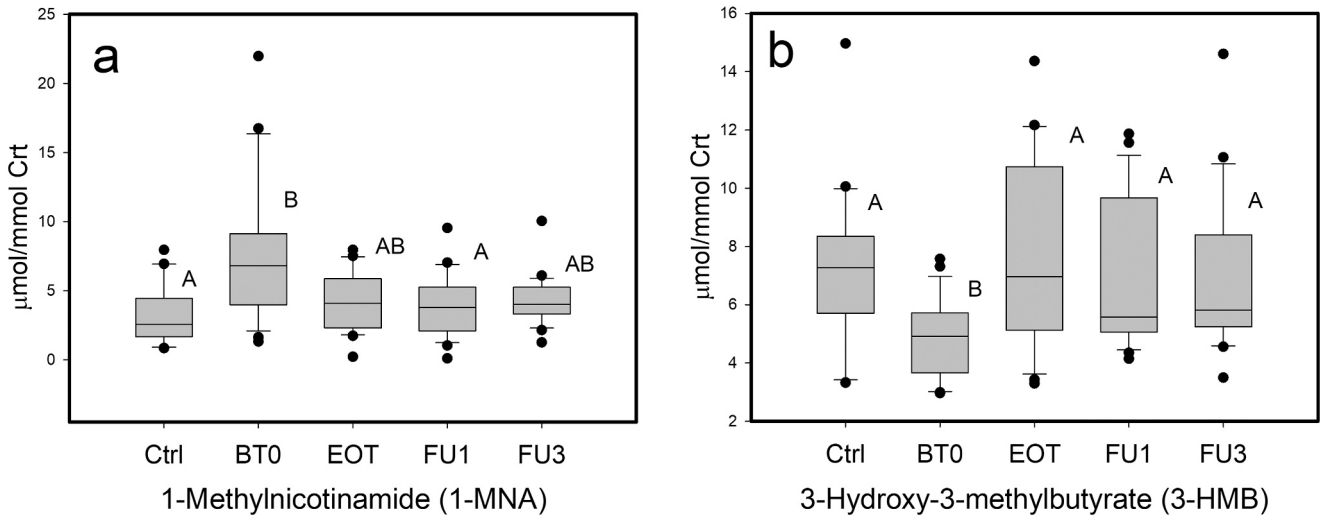

Fig. 5. Boxplot of urinary biomarkers associated with HCV clearance and SVR: a) 1-MNA, b) 3-HMB. Statistical significance was assessed by Kruskal-Wallis ANOVA on ranks test, using Bonferroni correction for P values (Dunn's method). P-value of 0.05 was considered as threshold for statistical significance, which is reported as letters (A or B or C) on the boxplots. Same letters indicate that there is no statistically significant difference, different letters indicate that there is a statistically significant difference among groups.

4.1. Urinary biomarkers correlated to severe liver fibrosis

The levels of PSI, hypoxanthine, MG, DMA, Gln and Tyr were systematically elevated in patients at BT0 and at EOT compared to Ctrl and remained unchanged through FU1 and FU3 (Fig. 4), suggesting that these metabolites could define the urinary profile of severe liver fibrosis, in spite of viral clearance induced by DAA treatment.

PSI is a post-transcriptionally modified nucleoside derived from ribosomal RNA and transfer RNA degradation and excreted in the urine without further modifications as an end product of RNA catabolism [Kegg map00240]. Its higher urinary levels reflect a high RNA turnover and hence a high protein turnover [21]. A study conducted in the era of interferon treatment for CHC showed that the levels of serum PSI were higher in CHC patients compared to healthy subjects and decreased significantly in subjects who achieved SVR [22]. However, our results show that PSI levels did not change with SVR, probably due to the different stage of liver disease, suggesting that the presence of an advanced liver disease could impair the recovery of this metabolic alteration. In addition, the increased levels of urinary PSI observed in NAFLD and obese children have been suggested to be related to the oxidative stress that increases protein turnover [23]. Therefore, we could speculate that the persistence of elevated PSI levels could be induced by a persistent state of oxidative stress in our patients despite SVR.

The increase of hypoxanthine levels suggests an alteration of purine metabolic pathway [Kegg map00230]. It has already been demonstrated that, in the context of severe liver disease, several reactive oxygen species (ROS) may be involved. Superoxide anion ($O2^{\cdot-}$) which is produced by different metabolic processes in vivo can be reduced by the enzyme superoxide dismutase (SOD) to hydrogen peroxide. Viral infection does not allow cells to handle pro-oxidant species, particularly in the liver, which have a detoxifying function from harmful substances [24]. The increased levels of hypoxanthine could be related to an increased serum activity of hypoxanthine oxygen-oxidoreductase (EC.: [1.17.3.2]) which catalyzes the reaction from xanthine and H_2O_2 to hypoxanthine, O_2 and H_2O, suggesting a compensatory mechanism for scavenging the hydrogen peroxide [25,26]. As for PSI levels, hypoxanthine concentrations remained persistently high during the study period and therefore it could be suggested as a potential biomarker of the chronic hepatic injury related to the oxidative stress.

MG was systematically higher in HCV patients compared to controls during the study period. In fact, MG is produced by the hepatic catabolism of creatinine and is regulated by active oxygen as a response to oxidative stress [27,28]. Furthermore, it has been shown that the synthesis of MG is co-occurrent with the synthesis of hydrogen peroxide in hepatic peroxisomes [29]. Since the function of peroxisomes is the scavenging of reactive oxygen species (ROS), an increase of MG could confirm the hypothesis of an altered oxidative state in fibrotic liver.

Finally, DMA is an intermediate of the catabolism of asymmetric dimethylarginine (ADMA), an endogenously produced amino acid that is a competitive inhibitor of nitric oxide synthase (NOS). ADMA is excreted unchanged into the urine (10%) and is metabolized by dimethylarginine dimethyl-amino-hydrolase (DDAH) to yield citrulline and DMA (90%), indeed the serum concentration of ADMA is negatively associated with hepatic DDAH activity [30,31]. ADMA is a mediator of endothelial dysfunction in animal models and in human cardiovascular and renal diseases [32]. High serum levels of ADMA have been reported in patients with cirrhosis and other severe liver diseases [33], and the increasing of ADMA levels could be involved in hepatic endothelial damage in liver inflammation and could be associated with portal hypertension in HCV cirrhosis [34,35].

PSI, hypoxanthine, MG and DMA seemed to characterize the urinary metabotype of chronic liver disease. Indeed, these changes were not restored by DAA therapy or viral clearance, and were persistently higher in patients with severe liver fibrosis after SVR. These metabolites are intermediates of different metabolic pathways, but all seem to be involved in mechanisms of response to ROS generated in the liver during the oxidative damages. ROS generated by chronic inflammation in HBV and HCV cirrhosis contribute to human hepatocarcinogenesis [36], therefore, it is very important to investigate more in depth the meaning of the observed variation in the levels of the metabolites in relation to the oxidative damage to define possible predictive and prognostic roles for the evolution of the liver disease.

The lack of targeted measurements of recognized oxidative stress biomarkers in urine or in serum could be a limitation of the present study to assess the persistence of an oxidative damage process during SVR. Nevertheless, our results suggest that treatment with antioxidant as an adjuvant intervention could be administered during or after DAA therapy.

Different considerations have to be made for the observed alterations of the amino acid metabolism such as Tyr and Gln. Chronic liver diseases is usually associated to an altered amino acid pattern, consisting of increased aromatic amino acids (AAA) and decreased branched amino acids (BCAA) concentrations, with a decreased Fisher's ratio (BCAA/

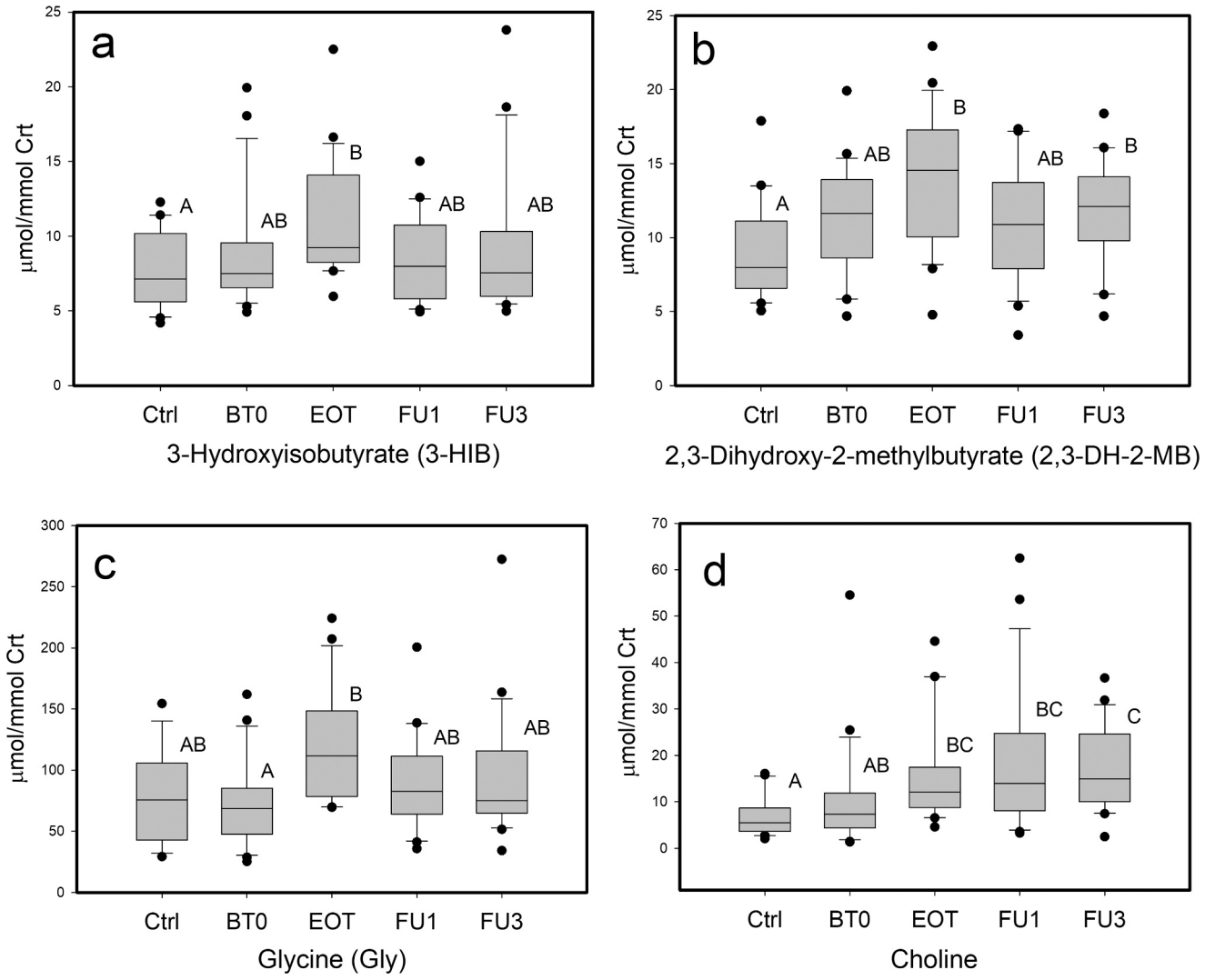

Fig. 6. Boxplot of urinary biomarkers related to DAA treatment: a) 3-HIB, b) 2,3-DH-2-MB, c) Gly, d) Choline. Statistical significance was assessed by Kruskal-Wallis ANOVA on ranks test, using Bonferroni correction for P values (Dunn's method). P-value of 0.05 was considered as threshold for statistical significance, which is reported as letters (A or B or C) on the boxplots. Same letters indicate that there is no statistically significant difference, different letters indicate that there is a statistically significant difference among groups.

AAA) [37,38]. These changes are caused by increased BCAA catabolism in muscles and decreased AAA breakdown in the diseased liver [39]. In our study, the observed high urinary Tyr levels and low valine to Tyr ratio in cirrhotic patients at baseline were in agreement with results previously obtained in blood [40]. Intriguingly, the baseline urinary levels of valine did not significantly differ between healthy controls and HCV-patients and only the Tyr and Gln levels were higher in HCV patients compared to the control group. Furthermore, the DAA treatment caused a further increase in Tyr levels that remained constant until FU3, while valine levels remained unchanged. Tyr levels are positively associated with HCC risk [41]; in addition, fluctuations of serum BCAA to Tyr ratio (BTR) are predicting prognosis in liver cirrhosis patients (death, worsening of esophageal and/or gastric varices, hepatocellular carcinoma and liver failure) [42,43], decreasing with increasing severity of hepatic damage [44]. Unfortunately, we were not able to determine the urinary concentration of leucine and isoleucine, and therefore we can only infer that a decrease of BTR ratio, due to an increase of Tyr levels, may occur after viral clearance in patients with advanced liver disease. If this is the case, BCAA supplementation therapy could be beneficial in HCV patients after viral clearance.

Finally, the higher Gln levels observed in patients compared to controls with a significant further increase during DAA treatment. In the context of severe liver fibrosis, ammonia accumulates through reduction of the hepatocyte functionality due to a reduction in liver cell mass [45]; therefore, the increased levels of Gln observed could be due to a persistent increased activity of Gln synthase (GS), which catalyzes the condensation of ammonia with glutamate (Glu) to produce Gln, contributing to both enteral and systemic ammonia detoxification [46].

4.2. Urinary metabolic biomarkers correlated to SVR

The levels of 1-MNA were significantly higher in HCV patients before DAA therapy compared to Ctrl and returned to normal levels at EOT (Fig. 5a), corresponding to viral clearance and normalization of serum liver enzymes. Increased plasma and urine concentrations of 1-MNA have been detected in HCV cirrhotic patients, due to an enhanced hepatic activity of nicotinamide-N-methyltransferase (NNMT) [47]. NNMT is a cytosolic enzyme localized mainly in the liver, which catalyzes the N-methylation of nicotinamide resulting in the synthesis of 1-MNA [48,49]. In the liver, the levels of 1-MNA mediated the metabolic effects of NNMT expression, which is positively correlated with hepatic inflammation parameters, Sirt1 activity and gluconeogenesis in primary hepatocytes, and negatively correlated with serum LDL [50]. The restoration of 1-MNA levels observed at EOT stage, and thus at HCV

clearance, occurred along with a significant reduction of transaminases levels, indirect markers of liver inflammation, and γGT levels, indirect marker of hepatic TNFα expression. A positive correlation between serum pro-inflammatory cytokine TNFα, severity of liver fibrosis and cirrhosis and HCV onset has also been found [51–54]. Therefore, our results confirmed the positive relation between 1-MNA levels and hepatic inflammation.

Intriguingly, the levels of 3-HMB, an intermediate of muscle catabolism of leucine [Kegg map00280], were lower before DAA treatment in HCV patients compared to Ctrl and their normal levels were restored at EOT without further changes during follow-up (Fig. 5b). 3-HMB is synthesized from leucine in a two-step process occurring in muscle and liver cells. The first step occurs through the reversible transfer of the leucine amino group to α-ketoglutarate (α-KG) to form glutamate and α-ketoisocaproate (α-KIC), catalyzed by muscle branched-chain-amino-acid aminotransferase (BCAT). The second step occurs through an irreversible oxidative decarboxylation of α-KIC, catalyzed by liver mithocondrial branched chain α-keto acid dehydrogenase (BCKDH) [55,56], leading to the formation of acetoacetate and acetyl-CoA, or by a cytosolic α-KIC dioxygenase leading to 3-HMB, then excreted by the kidneys (Fig. 7). 3-HMB has been demonstrated to stabilize the muscle cell membrane, to downregulate protein degradation and to upregulate protein synthesis, thus improving muscle mass, strength, function and physical performance in sarcopenic patients [57]. Although we could not determine the concentration of urinary leucine, this data could suggest that HCV clearance induces a normalization of muscle leucine catabolism and, consequently, an improvement of skeletal muscle protein synthesis.

4.3. Urinary metabolic biomarkers correlated to DAA therapy

The urinary levels of 3-HIB, 2,3-DH-2-MB, Gly and choline increased during the DAA treatment (Fig. 6).

In the skeletal muscle of cirrhotic patients, the reduced consumption of glucose leads to a compensatory energetic production through the utilization of BCAA [58]. Interestingly, the branched short chain acids (BSCA), such as 3-HIB and 2,3-DH-2-MB, are catabolic direct and indirect intermediates of valine metabolism, respectively. The catabolic pathway of valine is unique because mitochondrial methacrylyl-CoA (MC-CoA), a toxic compound, is produced in the middle part of the pathway and is detoxified in two steps by MC-CoA hydratase and 3-hydroxyisobutirril-CoA (HIBCH) hydrolases (Fig. 7). Therefore, the formation of 3-HIB is suggested to be physiologically important for protection of cells against the toxic effects of MC-CoA [59,60]. Interestingly, both enzymatic activities are very high in the healthy liver and significantly decreased in the cirrhotic liver, probably through a post-transcriptional regulation [61]. Furthermore, previous evidences indicated that 2,3-DH-2-MB could be formed from acryloyl CoA, produced from 3-HIB catabolism, through a mechanism yet not well clarified [59,62]. The increase in 2,3-DH-2-MB could be speculatively explained as an indirect effect of DAA on the control of the toxic acryloyl CoA levels in conditions of high valine muscle and liver catabolism and low flow through short-chain enoyl-CoA hydratase (ECHS1) or HIBCH [59] (Fig. 7). Unfortunately, we were unable to state if the increase of the toxic metabolite acryoyl CoA could be due to an alteration of the liver catabolic pathway of BSCA induced by DAAs, since microbiota contribution to the increase of valine intermediates cannot be excluded. If this hypothesis is correct, the administration of valine should be avoided during DAA treatment and should be administered, in association with other BCAAs, only after EOT.

Gly is a nonessential amino acid synthetized by several precursors and is the substrate of Glycine N-Methyl Transferase (GNMT) which catabolizes S-Adenosyl Methionine (SAM), the main methyl donor of the body. In order to maintain the homeostasis of SAM, sarcosine, the product of GNMT, can be transformed to Gly by sarcosine dehydrogenase (SDH) via oxidative demethylation [63]. It has been shown that patients with chronic liver disease often have reduced SAM biosynthesis [64]. On the contrary, our results showed that Gly levels significantly increased at EOT stage. This could be related to an increased activity of SDH to restore methionine and thus SAM balance, since it occurred along with a significant improvement of liver function tests during DAA treatment, with a significant decrease of transaminases values and with a restoration of 1-MNA levels (Fig. 8).

As observed for Gly, choline was significantly increased at EOT stage (Fig. 6d). Choline is involved in methyl group metabolism and its dietary deficiency has been shown to decrease S-adenosyl-L-methionine (SAM) levels and generate DNA hypomethylation, hepatic steatosis, cirrhosis, and HCC in rodents [65]. The higher urinary excretion of this metabolite at EOT stage further supports the hypothesis that DAAs could re-balance methionine metabolism acting on the methylation process (Fig. 8).

The increase of 3-HIB, 2,3-DH-2-MB and Gly levels appeared to be temporally related to DAA administration, as their levels returned to baseline at FU1 and FU3.

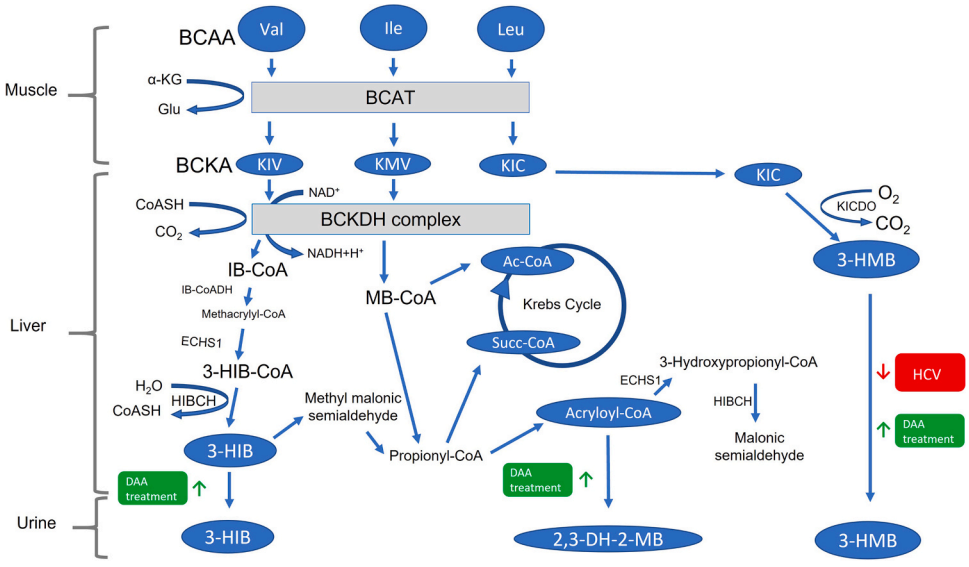

Fig. 7. Catabolic pathway of valine, isoleucine and leucine from muscles and liver to urinary excretion, proposed initially by Miyazaki et al. [55] and Fitzsimons et al. [61]. In red are indicated the pathways modifications induced by HCV and in green by DAA treatment. Val, Valine; Ile, Isoleucine; Leu, Leucine; BCAA, Branched-Chain Aminoacids; BCAT, Branched-Chain Aminotransferase; α-KG, α-Ketoglutarate; Glu, Glutamate; BCKA, branched-chain α-keto acids; KIV, α-Ketoisovalerate; KMV, α-Keto-β-methylvalerate; KIC, α-Ketoisocaproate; KICDO, KIC dioxygenase; Ac-CoA, Acetyl-CoA; Succ-CoA, Succynil-CoA; BCKDH complex, BCKA dehydrogenase complex; IB-CoA, Isobutyryl-CoA; 3-HIB-CoA, 3-Hydroxyisobutyryl-CoA; MB-CoA, α-methyl-butyryl-CoA; HIBCH, 3-HIB-CoA Hydrolase; ECHS1, Short-chain enoyl-CoA hydratase. For interpretation of the references to color in this figure legend, the reader is referred to the web version of this article.

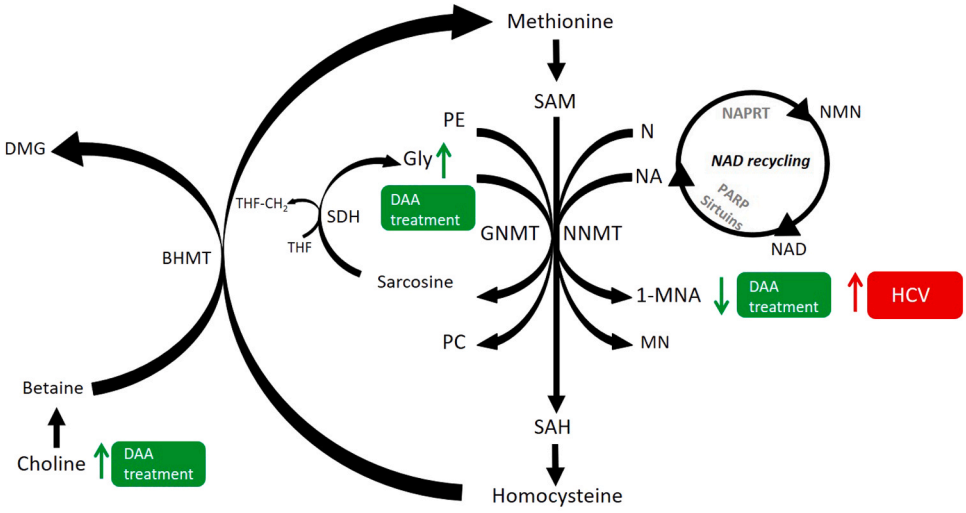

Fig. 8. Schematic representation of the transmethylation in the methionine and NAD metabolic pathways, based on the metabolite changes in urine of patients. In particular, green arrows indicates metabolite increased or decreased levels due to DAA treatment, while red arrow indicates 1-MNA increased levels due to HCV. 1-MNA, 1-methylnicotinamide; BHMT, betaine-homocysteine methyltransferase; Gly, glycine; GNMT, glycine N-methyltransferase; MN, methyl nicotinate; N, nicotinate; NA, nicotinamide; NAD, nicotinamide adenine dinucleotide; NAPRT, NA phosphoribosyltransferase; NMN: nicotinamide acid mononucleotide; NNMT, nicotinamide N-methyltransferase; PARP, poly (ADP-ribose) polymerases; PC, phosphatidylcholine; PE, phosphatidylethanolamine; SAH, S-adenosylhomocysteine; SAM, S-adenosylmethionine; SDH, sarcosine dehydrogenase; THF, tetrahydrofolate; THF-CH2, tetrahydrofolate methylene. For interpretation of the references to color in this figure legend, the reader is referred to the web version of this article.

5. Limitation of the study

The present study has some limitations. Firstly, the number of enrolled patients is small. Nevertheless, the PLS-DA models were extensively validated, and the observed differences were characterizing the metabotypes generated by HCV infection, severe fibrosis, SVR and DAA treatment. Secondly, in this study only male patients were considered, in order to limit the inter-individual variability and to have a more homogeneous sample. For these reasons, our results cannot be extended to females. Thirdly, the stage of liver fibrosis has not been assessed by liver biopsy, which is the gold standard. However, transient elastography has been demonstrated to be an accurate non-invasive technique to diagnose the presence of severe liver fibrosis or cirrhosis in HCV patients. Finally, regarding BCAA metabolism, we quantified valine but not leucine and isoleucine due to low concentration and overlapping of resonances, this limits the complete understanding of amino acids metabolism modifications occurring with DAAs administration and viral clearance.

6. Conclusions

This study represents the first investigation that monitors the metabolic changes occurring in HCV patients with severe liver fibrosis during DAA therapy and SVR by urinary ^{1}H NMR-based metabolomics and intriguing findings have been highlighted. Alterations in PSI, hypoxanthine, MG and DMA levels seem to be associated to oxidative stress in the context of advanced liver disease and, therefore, further studies could evaluate the potential benefit of an antioxidant treatment during or after DAA therapy. HCV clearance induces a normalization of muscle leucine catabolism and, possibly, an improvement of skeletal muscle protein synthesis. The restoration of 1-MNA levels observed at EOT stage could be related to the reduced hepatic inflammation. The type of amino acid supplementation in patients with severe liver fibrosis should be tailored to the changes of amino acid metabolism occurring during DAA therapy. The observed increase of Gly and choline could be related to a compensative mechanism involving in the SAM/SAH balance during DAA treatment.

Our preliminary results need to be confirmed by larger prospective study and should be correlated with clinical outcomes.

Financial support statement

The present research received a financial support by Sapienza University of Rome (Research Project 2017).

Author contributions

EB, OG, GT, and AM proposed and developed the research question, contributed to the study realization. AM, AT, FS, GC and OG performed laboratory evaluations. OG, GC, FS and FM did the data pre and post processing. FM performed the statistical analysis and statistical validation of the models. EB, OG, FS, FM, AT, DP, RE, MS, AM, GT interpreted the data and wrote the draft of the manuscript. All authors have seen and approved the final version of the manuscript. EB and OG contributed equally to the present study.

CRediT authorship contribution statement

Elisa Biliotti: Experimental work, Formal analysis, Investigation, Writing – original draft. **Ottavia Giampaoli:** Experimental work, Formal analysis, Investigation, Writing – original draft, Visualization. **Fabio Sciubba:** Formal analysis, Investigation, Writing – review & editing. **Federico Marini:** Software, Formal analysis, Visualization. **Alberta Tomassini:** Experimental work, Writing – original draft. **Donatella Palazzo:** Investigation, Data curation. **Giorgio Capuani:** Investigation, Formal analysis. **Rozenn Esvan:** Investigation, Data curation. **Martina Spaziante:** Investigation, Data curation. **Gloria Taliani:** Conceptualization, Supervision, Writing – review & editing, Project administration, Funding acquisition. **Alfredo Miccheli:** Conceptualization, Supervision, Methodology, Writing – review & editing. Elisa Biliotti and Ottavia Giampaoli contributed equally to this study Federico Marini did the multivariate statistical analysis, validated the models with repeated double cross validation method, did all the figures of merit, such as specificity, sensitivity, accuracy and AUROCs in the revised manuscript.

Declaration of competing interest

The authors have no conflicts of interest to declare. All co-authors have seen and agree with the contents of the present manuscript.

Appendix A. Supporting information

Supplementary data associated with this article can be found in the online version at doi:10.1016/j.biopha.2021.112217.

References

[1] S. Blach, S. Zeuzem, M. Manns, I. Altraif, A.-S. Duberg, D.H. Muljono, I. Waked, S. M. Alavian, M.-H. Lee, F. Negro, F. Abaalkhail, A. Abdou, M. Abdulla, A.A. Rached, I. Aho, U. Akarca, I. Al Ghazzawi, S. Al Kaabi, F. Al Lawati, K. Al Namaani, Y. Al Serkal, S.A. Al-Busafi, L. Al-Dabal, S. Aleman, A.S. Alghamdi, A.A. Aljumah, H. E. Al-Romaihi, M.I. Andersson, V. Arendt, P. Arkkila, A.M. Assiri, O. Baatarkhuu, A. Bane, Z. Ben-Ari, C. Bergin, F. Bessone, F. Bihl, A.R. Bizri, M. Blachier, A. J. Blasco, C.E.B. Mello, P. Andersson, C.R. Brunton, F. Calinas, H.L.Y. Chan, A. Chaudhry, H. Cheinquer, C.-J. Chen, R.-N. Chien, M.S. Choi, P.B. Christensen, W.-L. Chuang, V. Chulanov, L. Cisneros, M.R. Clausen, M.E. Cramp, A. Craxi, E. A. Croes, O. Dalgard, J.R. Daruich, V. de Ledinghen, G.J. Dore, M.H. El-Sayed, G. Ergör, G. Esmat, C. Estes, K. Falconer, E. Farag, M.L.G. Ferraz, P.R. Ferreira, R. Flisiak, S. Frankova, I. Gamkrelidze, E. Gane, J. García-Samaniego, A.G. Khan, I. Gountas, A. Goldis, M. Gottfredsson, J. Grebely, M. Gschwantler, M.G. Pessôa, J. Gunter, B. Hajarizadeh, O. Hajelssedig, S. Hamid, W. Hamoudi, A. Hatzakis, S. M. Himatt, H. Hofer, I. Hrstic, Y.-T. Hui, B. Hunyady, R. Idilman, W. Jafri, R. Jahis, N.Z. Janjua, P. Jarčuška, A. Jeruma, J.G. Jonasson, Y. Kamel, J.-H. Kao, S. Kaymakoglu, D. Kershenobich, J. Khamis, Y.S. Kim, L. Kondili, Z. Koutoubi, M. Krajden, H. Krarup, M. Lai, W. Laleman, W. Lao, D. Lavanchy, P. Lázaro, H. Leleu, O. Lesi, L.A. Lesmana, M. Li, V. Liakina, Y.-S. Lim, B. Luksic, A. Mahomed, M. Maimets, M. Makara, A.O. Malu, R.T. Marinho, P. Al Namaani, S. Mauss, M. S. Memon, M.C.M. Correa, N. Mendez-Sanchez, S. Merat, A.M. Metwally, R. Mohamed, C. Moreno, F.H. Mourad, B. Müllhaupt, K. Murphy, H. Nde, R. Njouom, D. Nonkovic, S. Al Serkal, S. Obekpa, S. Oguche, S. Olafsson, M. Oltman, O. Omede, C. Omuemu, O. Opare-Sem, A.L.H. Øvrehus, S. Owusu-Ofori, T.S. Oyunsuren, G. Papatheodoridis, K. Pasini, K.M. Peltekian, R.O. Phillips, N. Pimenov, H. Poustchi, N. Prabdial-Sing, H. Qureshi, A. Ramji, D. Razavi-Shearer, K. Razavi-Shearer, B. Redae, H.W. Reesink, E. Ridruejo, S. Robbins, L. R. Roberts, S.K. Roberts, W.M. Rosenberg, F. Roudot-Thoraval, S.D. Ryder, R. Safadi, O. Sagalova, R. Salupere, F.M. Sanai, J.F.S. Avila, V. Saraswat, R. Sarmento-Castro, C. Sarrazin, J.D. Schmelzer, I. Schréter, C. Seguin-Devaux, S. R. Shah, A.I. Sharara, M. Sharma, A. Shevaldin, G.E. Shiha, W. Sievert, M. Sonderup, K. Souliotis, D. Speiciene, J. Sperl, P. Stärkel, R.E. Stauber, C. Stedman, D. Struck, T.-H. Su, V. Sypsa, S.-S. Tan, J. Tanaka, A.J. Thompson, I. Tolmane, K. Tomasiewicz, J. Valantinas, P. Van Damme, A.J. van der Meer, I. van Thiel, H. Van Vlierberghe, A. Vince, W. Vogel, H. Wedemeyer, N. Weis, V.W. Wong, C. Yaghi, A. Yosry, M. Yuen, E. Yunihastuti, A. Yusuf, E. Zuckerman, H. Razavi, Global prevalence and genotype distribution of hepatitis C virus infection in 2015: a modelling study, Lancet Gastroenterol. Hepatol. 2 (2017) 161–176, https://doi.org/10.1016/S2468-1253(16)30181-9.

[2] A.P. Thrift, H.B. El-Serag, F. Kanwal, Global epidemiology and burden of HCV infection and HCV-related disease, Nat. Rev. Gastroenterol. Hepatol. 14 (2017) 122–132, https://doi.org/10.1038/nrgastro.2016.176.

[3] F. Negro, D. Forton, A. Craxì, M.S. Sulkowski, J.J. Feld, M.P. Manns, Extrahepatic morbidity and mortality of chronic hepatitis C, Gastroenterology 149 (2015) 1345–1360, https://doi.org/10.1053/j.gastro.2015.08.035.

[4] A.U. Neumann, N.P. Lam, H. Dahari, D.R. Gretch, T.E. Wiley, T.J. Layden, A. S. Perelson, Hepatitis C viral dynamics in vivo and the antiviral efficacy of interferon-alpha therapy, Science 282 (1998) 103–107, https://doi.org/10.1126/science.282.5386.103.

[5] T. Asselah, P. Marcellin, R.F. Schinazi, Treatment of hepatitis C virus infection with direct-acting antiviral agents: 100% cure? Liver Int. 38 (Suppl 1) (2018) 7–13, https://doi.org/10.1111/liv.13673.

[6] L.A. Kondili, G.B. Gaeta, M.R. Brunetto, A. Di Leo, A. Iannone, T.A. Santantonio, A. Giammario, G. Raimondo, R. Filomia, C. Coppola, D.C. Amoruso, P. Blanc, B. Del Pin, L. Chemello, L. Cavalletto, F. Morisco, L. Donnarumma, M.G. Rumi, A. Gasbarrini, M. Siciliano, M. Massari, R. Corsini, B. Coco, S. Madonia, M. Cannizzaro, A.L. Zignego, M. Monti, F.P. Russo, A. Zanetto, M. Persico, M. Masarone, E. Villa, V. Bernabucci, G. Taliani, E. Biliotti, L. Chessa, M.C. Pasetto, P. Andreone, M. Margotti, G. Brancaccio, D. Ieluzzi, G. Borgia, E. Zappulo, V. Calvaruso, S. Petta, L. Falzano, M.G. Quaranta, L.E. Weimer, S. Rosato, S. Vella, E.G. Giannini, Incidence of DAA failure and the clinical impact of retreatment in real-life patients treated in the advanced stage of liver disease: Interim evaluations from the PITER network, PLoS One 12 (2017), e0185728, https://doi.org/10.1371/journal.pone.0185728.

[7] V. Cento, T.H.T. Nguyen, D. Di Carlo, E. Biliotti, L. Gianserra, I. Lenci, D. Di Paolo, V. Calvaruso, E. Teti, M. Cerrone, D. Romagnoli, M. Melis, E. Danieli, B. Menzaghi, E. Polilli, M. Siciliano, L.A. Nicolini, A. Di Biagio, C.F. Magni, M. Bolis, F. P. Antonucci, V.C. Di Maio, R. Alfieri, L. Sarmati, P. Casalino, S. Bernardini, V. Micheli, G. Rizzardini, G. Parruti, T. Quirino, M. Puoti, S. Babudieri, A. D'Arminio Monforte, M. Andreoni, A. Craxì, M. Angelico, C. Pasquazzi, G. Taliani, J. Guedj, C.F. Perno, F. Ceccherini-Silberstein, Improvement of ALT decay kinetics by all-oral HCV treatment: role of NS5A inhibitors and differences with IFN-based regimens, PLoS One 12 (2017), e0177352, https://doi.org/10.1371/journal.pone.0177352.

[8] G.N. Ioannou, J.J. Feld, What are the benefits of a sustained virologic response to direct-acting antiviral therapy for hepatitis C virus infection? Gastroenterology 156 (2019) 446–460, https://doi.org/10.1053/j.gastro.2018.10.033.

[9] R. Amathieu, M.N. Triba, C. Goossens, N. Bouchemal, P. Nahon, P. Savarin, L. Le Moyec, Nuclear magnetic resonance based metabolomics and liver diseases: recent advances and future clinical applications, World J. Gastroenterol. 22 (2016) 417–426, https://doi.org/10.3748/wjg.v22.i1.417.

[10] N.G. Ladep, A.C. Dona, M.R. Lewis, M.M.E. Crossey, M. Lemoine, E. Okeke, Y. Shimakawa, M. Duguru, H.F. Njai, H.K.S. Fye, M. Taal, J. Chetwood, B. Kasstan, S.A. Khan, D.A. Garside, A. Wijeyesekera, A.V. Thillainayagam, E. Banwat, M. R. Thursz, J.K. Nicholson, R. Njie, E. Holmes, S.D. Taylor-Robinson, Discovery and validation of urinary metabotypes for the diagnosis of hepatocellular carcinoma in West Africans, Hepatology 60 (2014) 1291–1301, https://doi.org/10.1002/hep.27264.

[11] M.M.G. Godoy, E.P.A. Lopes, R.O. Silva, F. Hallwass, L.C.A. Koury, I.M. Moura, S. M.C. Gonçalves, A.M. Simas, Hepatitis C virus infection diagnosis using metabonomics, J. Viral Hepat. 17 (2010) 854–858, https://doi.org/10.1111/j.1365-2893.2009.01252.x.

[12] Z. Schofield, M.A. Reed, P.N. Newsome, D.H. Adams, U.L. Günther, P.F. Lalor, Changes in human hepatic metabolism in steatosis and cirrhosis, World J. Gastroenterol. 23 (2017) 2685–2695, https://doi.org/10.3748/wjg.v23.i15.2685.

[13] N. Embade, Z. Mariño, T. Diercks, A. Cano, S. Lens, D. Cabrera, M. Navasa, J. M. Falcón-Pérez, J. Caballería, A. Castro, J. Bosch, J.M. Mato, O. Millet, Metabolic characterization of advanced liver fibrosis in HCV patients as studied by serum ^{1}H NMR spectroscopy, PLoS One 11 (2016), e0155094, https://doi.org/10.1371/journal.pone.0155094.

[14] T. Gabbani, M. Marsico, P. Bernini, E. Lorefice, C. Grappone, M.R. Biagini, S. Milani, V. Annese, Metabolomic analysis with ^{1}H NMR for non-invasive diagnosis of hepatic fibrosis degree in patients with chronic hepatitis C, Dig. Liver Dis. 49 (2017) 1338–1344, https://doi.org/10.1016/j.dld.2017.05.018.

[15] G. Meoni, S. Lorini, M. Monti, F. Madia, G. Corti, C. Luchinat, A.L. Zignego, L. Tenori, L. Gragnani, The metabolic fingerprints of HCV and HBV infections studied by Nuclear Magnetic Resonance Spectroscopy, Sci. Rep. 9 (2019) 4128, https://doi.org/10.1038/s41598-019-40028-4.

[16] L. Castéra, J. Vergniol, J. Foucher, B. Le Bail, E. Chanteloup, M. Haaser, M. Darriet, P. Couzigou, V. De Lédinghen, Prospective comparison of transient elastography, Fibrotest, APRI, and liver biopsy for the assessment of fibrosis in chronic hepatitis C, Gastroenterology 128 (2005) 343–350, https://doi.org/10.1053/j.gastro.2004.11.018.

[17] E. Brasili, E. Mengheri, A. Tomassini, G. Capuani, M. Roselli, A. Finamore, F. Sciubba, F. Marini, A. Miccheli, Lactobacillus acidophilus La5 and Bifidobacterium lactis Bb12 induce different age-related metabolic profiles revealed by ^{1}H NMR spectroscopy in urine and feces of mice, J. Nutr. 143 (2013) 1549–1557, https://doi.org/10.3945/jn.113.177105.

[18] E. Szymańska, E. Saccenti, A.K. Smilde, J.A. Westerhuis, Double-check: validation of diagnostic statistics for PLS-DA models in metabolomics studies, Metabolomics 8 (2012) 3–16, https://doi.org/10.1007/s11306-011-0330-3.

[19] C. Di Poto, A. Ferrarini, Y. Zhao, R.S. Varghese, C. Tu, Y. Zuo, M. Wang, M. R. Nezami Ranjbar, Y. Luo, C. Zhang, C.S. Desai, K. Shetty, M.G. Tadesse, H. W. Ressom, Metabolomic characterization of hepatocellular carcinoma in patients with liver cirrhosis for biomarker discovery, Cancer Epidemiol. Biomark. Prev. 26 (2017) 675–683, https://doi.org/10.1158/1055-9965.EPI-16-0366.

[20] X. Wang, A. Zhang, H. Sun, Power of metabolomics in diagnosis and biomarker discovery of hepatocellular carcinoma, Hepatology 57 (2013) 2072–2077, https://doi.org/10.1002/hep.26130.

[21] G. Schöch, H. Topp, A. Held, G. Heller-Schöch, A. Ballauff, F. Manz, G. Sander, Interrelation between whole-body turnover rates of RNA and protein, Eur. J. Clin. Nutr. 44 (1990) 647–658.

[22] A. Colonna, V. Guadagnino, A. Maiorano, E. Stamile, C. Costa, Pseudouridine for monitoring interferon treatment of patients with chronic hepatitis C, Eur. J. Clin. Chem. Clin. Biochem 34 (1996) 697–700, https://doi.org/10.1515/cclm.1996.34.9.697.

[23] A. Miccheli, G. Capuani, F. Marini, A. Tomassini, G. Praticò, S. Ceccarelli, D. Gnani, G. Baviera, A. Alisi, L. Putignani, V. Nobili, Urinary (1)H NMR-based metabolic profiling of children with NAFLD undergoing VSL#3 treatment, Int J. Obes. 39 (2015) 1118–1125, https://doi.org/10.1038/ijo.2015.40.

[24] U.Z. Paracha, K. Fatima, M. Alqahtani, A. Chaudhary, A. Abuzenadah, G. Damanhouri, I. Qadri, Oxidative stress and hepatitis C virus, Virol. J. 10 (2013) 251, https://doi.org/10.1186/1743-422X-10-251.

[25] G. Nalini, C. Hariprasad, V.A. Narayanan, Oxidative stress in alcoholic liver disease, Indian J. Med Res. 110 (1999) 200–203.

[26] P. Toledo-Ibelles, R. Gutiérrez-Vidal, S. Calixto-Tlacomulco, B. Delgado-Coello, J. Mas-Oliva, Hepatic accumulation of hypoxanthine: a link between hyperuricemia and nonalcoholic fatty liver disease, Arch. Med. Res. (2021), https://doi.org/10.1016/j.arcmed.2021.04.005.

[27] K. Nakamura, K. Ienaga, T. Yokozawa, N. Fujitsuka, H. Oura, Production of methylguanidine from creatinine via creatol by active oxygen species: analyses of the catabolism in vitro, Nephron 58 (1991) 42–46, https://doi.org/10.1159/000186376.

[28] K. Aoyagi, S. Nagase, M. Narita, S. Tojo, Role of active oxygen on methylguanidine synthesis in isolated rat hepatocytes, Kidney Int. Suppl. 22 (1987) S229–S233.

[29] K. Takemura, K. Aoyagi, S. Nagase, M. Gotoh, A. Hirayama, A. Ueda, C. Tomida, A. Koyama, Biosynthesis of methylguanidine in the hepatic peroxisomes and the effect of the induction of peroxisomal enzymes by clofibrate, NEF 78 (1998) 82–87, https://doi.org/10.1159/000044886.

[30] J. Leiper, M. Nandi, B. Torondel, J. Murray-Rust, M. Malaki, B. O'Hara, S. Rossiter, S. Anthony, M. Madhani, D. Selwood, C. Smith, B. Wojciak-Stothard, A. Rudiger, R. Stidwill, N.Q. McDonald, P. Vallance, Disruption of methylarginine metabolism

impairs vascular homeostasis, Nat. Med. 13 (2007) 198–203, https://doi.org/10.1038/nm1543.
[31] M. Davids, M.C. Richir, M. Visser, B. Ellger, G. van den Berghe, P.A.M. van Leeuwen, T. Teerlink, Role of dimethylarginine dimethylaminohydrolase activity in regulation of tissue and plasma concentrations of asymmetric dimethylarginine in an animal model of prolonged critical illness, Metabolism 61 (2012) 482–490, https://doi.org/10.1016/j.metabol.2011.08.007.
[32] S. Blackwell, The biochemistry, measurement and current clinical significance of asymmetric dimethylarginine, Ann. Clin. Biochem. 47 (2010) 17–28, https://doi.org/10.1258/acb.2009.009196.
[33] P. Lluch, G. Segarra, P. Medina, Asymmetric dimethylarginine as a mediator of vascular dysfunction in cirrhosis, World J. Gastroenterol. 21 (2015) 9466–9475, https://doi.org/10.3748/wjg.v21.i32.9466.
[34] B. Vairappan, Endothelial dysfunction in cirrhosis: role of inflammation and oxidative stress, World J. Hepatol. 7 (2015) 443–459, https://doi.org/10.4254/wjh.v7.i3.443.
[35] F. Vizzutti, R.G. Romanelli, U. Arena, L. Rega, M. Brogi, C. Calabresi, E. Masini, R. Tarquini, M. Zipoli, V. Boddi, F. Marra, G. Laffi, M. Pinzani, ADMA correlates with portal pressure in patients with compensated cirrhosis, Eur. J. Clin. Invest. 37 (2007) 509–515, https://doi.org/10.1111/j.1365-2362.2007.01814.x.
[36] C. Jüngst, B. Cheng, R. Gehrke, V. Schmitz, H.D. Nischalke, J. Ramakers, P. Schramel, P. Schirmacher, T. Sauerbruch, W.H. Caselmann, Oxidative damage is increased in human liver tissue adjacent to hepatocellular carcinoma, Hepatology 39 (2004) 1663–1672, https://doi.org/10.1002/hep.20241.
[37] C.H.C. Dejong, M.C.G. van de Poll, P.B. Soeters, R. Jalan, S.W.M.Olde Damink, Aromatic amino acid metabolism during liver failure, J. Nutr. 137 (2007) 1579S–1585S, https://doi.org/10.1093/jn/137.6.1579S.
[38] T. Kawaguchi, N. Izumi, M.R. Charlton, M. Sata, Branched-chain amino acids as pharmacological nutrients in chronic liver disease, Hepatology 54 (2011) 1063–1070, https://doi.org/10.1002/hep.24412.
[39] M. Holecek, Ammonia and amino acid profiles in liver cirrhosis: effects of variables leading to hepatic encephalopathy, Nutrition 31 (2015) 14–20, https://doi.org/10.1016/j.nut.2014.03.016.
[40] T.M. Devlin. Textbook of Biochemistry with Clinical Correlations, seventh ed., John Wiley & Sons, 2010.
[41] M. Stepien, T. Duarte-Salles, V. Fedirko, A. Floegel, D.K. Barupal, S. Rinaldi, D. Achaintre, N. Assi, A. Tjønneland, K. Overvad, N. Bastide, M.-C. Boutron-Ruault, G. Severi, T. Kühn, R. Kaaks, K. Aleksandrova, H. Boeing, A. Trichopoulou, C. Bamia, P. Lagiou, C. Saieva, C. Agnoli, S. Panico, R. Tumino, A. Naccarati, H.B. A. Bueno-de-Mesquita, P.H. Peeters, E. Weiderpass, J.R. Quirós, A. Agudo, M.-J. Sánchez, M. Dorronsoro, D. Gavrila, A. Barricarte, B. Ohlsson, K. Sjöberg, M. Werner, M. Sund, N. Wareham, K.-T. Khaw, R.C. Travis, J.A. Schmidt, M. Gunter, A. Cross, P. Vineis, I. Romieu, A. Scalbert, M. Jenab, Alteration of amino acid and biogenic amine metabolism in hepatobiliary cancers: findings from a prospective cohort study, Int. J. Cancer 138 (2016) 348–360, https://doi.org/10.1002/ijc.29718.
[42] B. Kinny-Köster, M. Bartels, S. Becker, M. Scholz, J. Thiery, U. Ceglarek, T. Kaiser, Plasma amino acid concentrations predict mortality in patients with end-stage liver disease, PLoS One 11 (2016), e0159205, https://doi.org/10.1371/journal.pone.0159205.
[43] T. Kawaguchi, K. Shiraishi, T. Ito, K. Suzuki, C. Koreeda, T. Ohtake, M. Iwasa, Y. Tokumoto, R. Endo, N. Kawamura, M. Shiraki, D. Habu, S. Tsuruta, Y. Miwa, A. Kawaguchi, T. Kakuma, H. Sakai, N. Kawada, T. Hanai, S. Takahashi, A. Kato, M. Onji, Y. Takei, Y. Kohgo, T. Seki, M. Tamano, K. Katayama, T. Mine, M. Sata, H. Moriwaki, K. Suzuki, Branched-chain amino acids prevent hepatocarcinogenesis and prolong survival of patients with cirrhosis, Clin. Gastroenterol. Hepatol. 12 (2014) 1012–1018, https://doi.org/10.1016/j.cgh.2013.08.050.
[44] T. Ishikawa, M. Imai, M. Ko, H. Sato, Y. Nozawa, T. Sano, A. Iwanaga, K. Seki, T. Honma, T. Yoshida, Evaluation of the branched-chain amino acid-to-tyrosine ratio prior to treatment as a prognostic predictor in patients with liver cirrhosis, Oncotarget 8 (2017) 79480–79490, https://doi.org/10.18632/oncotarget.18447.
[45] K.L. Thomsen, F. De Chiara, K. Rombouts, H. Vilstrup, F. Andreola, R.P. Mookerjee, R. Jalan, Ammonia:a novel target for the treatment of non-alcoholic steatohepatitis, Med. Hypotheses 113 (2018) 91–97, https://doi.org/10.1016/j.mehy.2018.02.010.
[46] Y. Zhou, T. Eid, B. Hassel, N.C. Danbolt, Novel aspects of glutamine synthetase in ammonia homeostasis, Neurochem. Int. 140 (2020), 104809, https://doi.org/10.1016/j.neuint.2020.104809.
[47] R. Cuomo, M. Dattilo, R. Pumpo, G. Capuano, L. Boselli, G. Budillon, Nicotinamide methylation in patients with cirrhosis, J. Hepatol. 20 (1994) 138–142, https://doi.org/10.1016/s0168-8278(05)80480-5.
[48] S. Aksoy, C.L. Szumlanski, R.M. Weinshilboum, Human liver nicotinamide N-methyltransferase. cDNA cloning, expression, and biochemical characterization, J. Biol. Chem. 269 (1994) 14835–14840.
[49] P. Pissios, Nicotinamide N-methyltransferase: more than a vitamin B3 clearance enzyme, Trends Endocrinol. Metab. 28 (2017) 340–353, https://doi.org/10.1016/j.tem.2017.02.004.
[50] S. Hong, J.M. Moreno-Navarrete, X. Wei, Y. Kikukawa, I. Tzameli, D. Prasad, Y. Lee, J.M. Asara, J.M. Fernandez-Real, E. Maratos-Flier, P. Pissios, Nicotinamide N-methyltransferase regulates hepatic nutrient metabolism through Sirt1 protein stabilization, Nat. Med. 21 (2015) 887–894, https://doi.org/10.1038/nm.3882.
[51] M.J. Koziel, Cytokines in viral hepatitis, Semin Liver Dis. 19 (1999) 157–169, https://doi.org/10.1055/s-2007-1007107.
[52] H. Zylberberg, A.-C. Rimaniol, S. Pol, A. Masson, D.D. Groote, P. Berthelot, J.-F. Bach, C. Bréchot, F. Zavala, Soluble tumor necrosis factor receptors in chronic hepatitis C: a correlation with histological fibrosis and activity, J. Hepatol. 30 (1999) 185–191, https://doi.org/10.1016/S0168-8278(99)80060-9.
[53] Z. Wang, A. Wang, Z. Gong, I. Biviano, H. Liu, J. Hu, Plasma claudin-3 is associated with tumor necrosis factor-alpha-induced intestinal endotoxemia in liver disease, Clin. Res. Hepatol. Gastroenterol. 43 (2019) 410–416, https://doi.org/10.1016/j.clinre.2018.11.014.
[54] D.R. Nelson, H.L. Lim, C.G. Marousis, J.W.S. Fang, G.L. Davis, L. Shen, M.S. Urdea, J.A. Kolberg, J.Y.N. Lau, Activation of tumor necrosis factor-α system in chronic hepatitis C virus infection, Dig. Dis. Sci. 42 (1997) 2487–2494, https://doi.org/10.1023/A:1018804426724.
[55] R. Rajendram, V.R. Preedy, V.B. Patel (Eds.), Branched Chain Amino Acids in Clinical Nutrition: Volume 1, Humana Press, 2015, https://doi.org/10.1007/978-1-4939-1923-9.
[56] T. Miyazaki, A. Honda, T. Ikegami, J. Iwamoto, T. Monma, T. Hirayama, Y. Saito, K. Yamashita, Y. Matsuzaki, Simultaneous quantification of salivary 3-hydroxybutyrate, 3-hydroxyisobutyrate, 3-hydroxy-3-methylbutyrate, and 2-hydroxybutyrate as possible markers of amino acid and fatty acid catabolic pathways by LC–ESI–MS/MS, SpringerPlus 4 (2015) 494, https://doi.org/10.1186/s40064-015-1304-0.
[57] F. Landi, R. Calvani, A. Picca, E. Marzetti, Beta-hydroxy-beta-methylbutyrate and sarcopenia: from biological plausibility to clinical evidence, Curr. Opin. Clin. Nutr. Metab. Care 22 (2019) 37–43, https://doi.org/10.1097/MCO.0000000000000524.
[58] H. Moriwaki, Y. Miwa, M. Tajika, M. Kato, H. Fukushima, M. Shiraki, Branched-chain amino acids as a protein- and energy-source in liver cirrhosis, Biochem. Biophys. Res. Commun. 313 (2004) 405–409, https://doi.org/10.1016/j.bbrc.2003.07.016.
[59] H. Peters, S. Ferdinandusse, J.P. Ruiter, R.J.A. Wanders, A. Boneh, J. Pitt, Metabolite studies in HIBCH and ECHS1 defects: implications for screening, Mol. Genet. Metab. 115 (2015) 168–173, https://doi.org/10.1016/j.ymgme.2015.06.008.
[60] K. Taniguchi, T. Nonami, A. Nakao, A. Harada, T. Kurokawa, S. Sugiyama, N. Fujitsuka, Y. Shimomura, S.M. Hutson, R.A. Harris, H. Takagi, The valine catabolic pathway in human liver: effect of cirrhosis on enzyme activities, Hepatology 24 (1996) 1395–1398, https://doi.org/10.1002/hep.510240614.
[61] Y. Shimomura, T. Honda, H. Goto, T. Nonami, T. Kurokawa, M. Nagasaki, T. Murakami, Effects of liver failure on the enzymes in the branched-chain amino acid catabolic pathway, Biochem. Biophys. Res. Commun. 313 (2004) 381–385, https://doi.org/10.1016/j.bbrc.2003.07.022.
[62] P.E. Fitzsimons, C.L. Alston, P.E. Bonnen, J. Hughes, E. Crushell, M.T. Geraghty, M. Tetreault, P. O'Reilly, E. Twomey, Y. Sheikh, R. Walsh, H.R. Waterham, S. Ferdinandusse, R.J.A. Wanders, R.W. Taylor, J.J. Pitt, P.D. Mayne, Clinical, biochemical, and genetic features of four patients with short-chain enoyl-CoA hydratase (ECHS1) deficiency, Am. J. Med. Genet. A 176 (2018) 1115–1127, https://doi.org/10.1002/ajmg.a.38658.
[63] J.M. Mato, M.L. Martínez-Chantar, S.C. Lu, S-adenosylmethionine metabolism and liver disease, Ann. Hepatol. 12 (2013) 183–189, https://doi.org/10.1016/S1665-2681(19)31355-9.
[64] Q.M. Anstee, C.P. Day, S-adenosylmethionine (SAMe) therapy in liver disease: a review of current evidence and clinical utility, J. Hepatol. 57 (2012) 1097–1109, https://doi.org/10.1016/j.jhep.2012.04.041.
[65] C.D. Davis, E.O. Uthus, DNA methylation, cancer susceptibility, and nutrient interactions, Exp. Biol. Med. 229 (2004) 988–995, https://doi.org/10.1177/153537020422901002.